

New Derivatives of PCP-Type Pincer Complexes of Nickel

Annie Castonguay, André L. Beauchamp, and Davit Zargarian*

Département de Chimie, Université de Montréal, Montréal, Québec H3C 3J7, Canada

Received August 27, 2008

The pincer-type complexes $(PC_{sp^3}P^{iPr})NiR$ ($PC_{sp^3}P^{iPr} = (iPr)_2PCH_2CH_2CH$) react with HBF_4 ($R = C\equiv Me$, Ph, Me) or $AgBF_4$ ($R = Br$) to give $(PC_{sp^3}P^{iPr})Ni(BF_4)$, **1**, which was found to involve fluxional Ni–F–BF₃ interactions. Competition experiments revealed that the relative ease of protonation of the Ni–hydrocarbyl moiety follows the order Ni–Me > Ni–C≡Me > Ni–Ph. Complex **1** reacts with water to give $[(PC_{sp^3}P^{iPr})Ni(H_2O)][BF_4]$, **2**, that in turn undergoes H₂O exchange with CH₃CN, *i*-PrNH₂, and CO to give the corresponding cationic adducts **3**, **4**, and **5**; alternatively, **3–5** can also be obtained directly from the reaction of **1** with CH₃CN, *i*-PrNH₂, and CO, respectively. Deprotonation of complex **2** gives the neutral hydroxo complex $(PC_{sp^3}P^{iPr})Ni(OH)$, **6**. All complexes have been characterized by NMR spectroscopy and, in the case of **2–6**, by X-ray crystallography.

Introduction

Most PCP-type pincer complexes¹ of late transition metals are well-known for their air-, water-, and thermal-stabilities and the numerous catalytic reactions they promote.² The most extensively investigated complexes feature ligands based on a *meta*-disubstituted arene skeleton ($PC_{sp^2}P$), but ligands based on an aliphatic skeleton and an sp^3 -hybridized metallated carbon atom ($PC_{sp^3}P$) are becoming popular since it has been demonstrated that their complexes possess enhanced or unique reactivities. For example, the $(PC_{sp^3}P)$ -Pd complex $\kappa^P, \kappa^C, \kappa^P$ -{1-CH₂-2,6-(CH₂P(*i*-Pr))₂-3,5-(CH₃)₂-C₆H}Pd (O₂CCF₃) is a more active precatalyst for the Heck coupling in comparison to its corresponding $(PC_{sp^2}P)$ -Pd analogue,³

some $(PC_{sp^3}P)$ -Ir complexes facilitate alkane metathesis⁴ and activate the N–H bond of ammonia⁵ and the C–H bond of benzene,⁶ while a $(PC_{sp^3}P)$ -Os complex has allowed the stabilization of a rare silylene species.⁷

We are interested in exploring the reactivities of PCP-Ni complexes in catalytic transformations. The first such complexes to be reported in the literature were based on a $PC_{sp^2}P$ framework (Chart 1),⁸ but an increasing number of $PC_{sp^3}P$ -based complexes of nickel have appeared in the literature over the past few years, including $\kappa^P, \kappa^C, \kappa^P$ -{1-CH₂-2,6-(CH₂P(*i*-Pr))₂-3,5-(CH₃)₂-C₆H}Ni^{II} and $[(PC_{sp^3}P^{iBu})NiL]^{n+}$ ($PC_{sp^3}P^{iBu} = (t-Bu)_2PCH_2CH_2CH$; $n = 0$: L = Cl, Br, I, H, Me; $n = 1$: L = MeCN, CH₂=CHCN).⁹ Very recently, we have introduced a new series of Ni^{II} and Ni^{III}

* To whom correspondence should be addressed. E-mail: zargarian.davit@umontreal.ca.

- (1) For some of the original reports on PCP type pincer complexes see: (a) Moulton, C. J.; Shaw, B. L. *Dalton Trans.* **1976**, 1020. (b) Al-Salem, N. A.; Empsall, H. D.; Markham, R.; Shaw, B. L.; Weeks, B. *Dalton Trans.* **1979**, 1972. (c) Al-Salem, N. A.; McDonald, W. S.; Markham, R.; Norton, M. C.; Shaw, B. L. *Dalton Trans.* **1980**, 59. (d) Crocker, C.; Errington, R. J.; Markham, R.; Moulton, C. J.; Odell, K. J.; Shaw, B. L. *J. Am. Chem. Soc.* **1980**, 102, 4373. (e) Crocker, C.; Errington, R. J.; Markham, R.; Moulton, C. J.; Shaw, B. L. *Dalton Trans.* **1982**, 387. (f) Crocker, C.; Empsall, H. D.; Errington, R. J.; Hyde, E. M.; McDonald, W. S.; Markham, R.; Norton, M. C.; Shaw, B. L.; Weeks, B. *Dalton Trans.* **1982**, 1217. (g) Briggs, J. R.; Constable, A. G.; McDonald, W. S.; Shaw, B. L. *Dalton Trans.* **1982**, 1225.
- (2) (a) Albrecht, M.; van Koten, G. *Angew. Chem., Int. Ed.* **2001**, 40, 3750. (b) van der Boom, M. E.; Milstein, D. *Chem. Rev.* **2003**, 103, 1759. (c) Singleton, J. T. *Tetrahedron* **2003**, 59, 1837.
- (3) Ohff, M.; Ohff, A.; van der Boom, M. E.; Milstein, D. *J. Am. Chem. Soc.* **1997**, 119, 11687.

(4) Goldman, A. S.; Roy, A. H.; Huang, Z.; Ahuja, R.; Schinski, W.; Brookhart, M. *Science* **2006**, 312, 257.

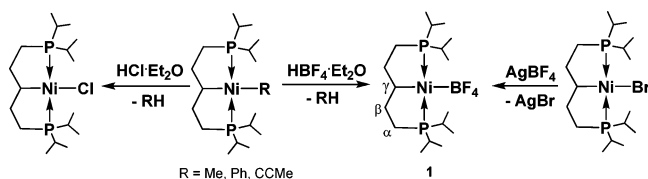
(5) Zhao, J.; Goldman, A. S.; Hartwig, J. F. *Science* **2005**, 307, 1080.

(6) Kanzelberger, M.; Singh, B.; Czerw, M.; Krogh-Jespersen, K.; Goldman, A. S. *J. Am. Chem. Soc.* **2000**, 122, 11017.

(7) Gusev, D. G.; Fonatine, F.-G.; Lough, A. J.; Zargarian, D. *Angew. Chem., Int. Ed.* **2003**, 42, 216.

(8) For examples of Ni– $PC_{sp^2}P$ complexes see ref 1a and the following reports: (a) Kennedy, A. R.; Cross, R. J.; Muir, K. W. *Inorg. Chim. Acta* **1995**, 231, 195. (b) Huck, W. T. S.; Snellink-Ruël, B.; van Veggel, F. C. J. M.; Reinhoudt, D. N. *Organometallics* **1997**, 16, 4287. (c) Bachechi, F. *Struct. Chem.* **2003**, 14, 263. (d) Kozhanov, K. A.; Bubnov, M. P.; Cherkasov, V. K.; Fukin, G. K.; Abakumov, G. A. *Chem. Commun.* **2003**, 2610. (e) Kozhanov, K. A.; Bubnov, M. P.; Cherkasov, V. K.; Fukin, G. K.; Abakumov, G. A. *Dalton Trans.* **2004**, 2957. (f) Cámpora, J.; Palma, P.; del Río, D.; Álvarez, E. *Organometallics* **2004**, 23, 1652. (g) Cámpora, J.; Palma, P.; del Río, D.; Conejo, M. M.; Álvarez, E. *Organometallics* **2004**, 23, 5653. (h) van der Boom, M. E.; Liou, S. Y.; Shimon, L. J. W.; Ben-David, Y.; Milstein, D. *Inorg. Chim. Acta* **2004**, 357, 4015. (i) Groux, L. F.; Bélanger-Gariépy, F.; Zargarian, D. *Can. J. Chem.* **2005**, 83, 634.

Scheme 1



complexes based on the ligand $\text{PC}_{\text{sp}^3}\text{P}^{\text{i-Pr}}$ ($\text{PC}_{\text{sp}^3}\text{P}^{\text{i-Pr}} = (i\text{-Pr}_2\text{PCH}_2\text{CH}_2)_2\text{CH}$), and studied their structural characteristics and reactivities.¹⁰

Our investigations have revealed significant structural and reactivity differences among Ni complexes based on $\text{PC}_{\text{sp}^2}\text{P}$ versus $\text{PC}_{\text{sp}^3}\text{P}$ and $\text{PC}_{\text{sp}^3}\text{P}^{\text{i-Bu}}$ versus $\text{PC}_{\text{sp}^3}\text{P}^{\text{i-Pr}}$ ligands.¹¹ For example, we have found^{10b} that $(\text{PC}_{\text{sp}^3}\text{P}^{\text{i-Pr}})\text{Ni}(\text{Bu})$ is quite stable to $\beta\text{-H}$ elimination, in contrast to its $\text{PC}_{\text{sp}^3}\text{P}^{\text{i-Bu}}$ analogue. Moreover, whereas $(\text{PC}_{\text{sp}^3}\text{P}^{\text{i-Pr}})\text{NiBr}$ is an efficient catalyst for the Corriu–Kumada coupling of MeMgCl and PhCl , the $\text{PC}_{\text{sp}^2}\text{P}^{\text{i-Pr}}$ analogue of this complex was found to be almost completely inactive under the same conditions. Finally, it has been possible to isolate a thermally stable $(\text{PC}_{\text{sp}^3}\text{P}^{\text{i-Pr}})\text{Ni}^{\text{III}}\text{Br}_2$ species,^{10b} whereas no trivalent complexes of the analogous $\text{PC}_{\text{sp}^2}\text{P}$ ligands have been isolated to date.^{12,13}

During the course of our studies on the reactivities of PCP-Ni complexes, we have found that protonolysis of $(\text{PC}_{\text{sp}^3}\text{P}^{\text{i-Pr}})\text{Ni}(\text{hydrocarbyl})$ with HBF_4 gives the Ni-BF_4 derivative $(\text{PC}_{\text{sp}^3}\text{P}^{\text{i-Pr}})\text{Ni}(\text{BF}_4)$, **1**, a species which appears to involve weak Ni-F-BF_3 interactions. The present report describes the characterization of this new compound and its use as a precursor for the preparation of $[(\text{PC}_{\text{sp}^3}\text{P}^{\text{i-Pr}})\text{Ni}(\text{L})][\text{BF}_4]$ ($\text{L} = \text{H}_2\text{O}$ (**2**), CH_3CN (**3**), $i\text{-PrNH}_2$ (**4**), CO (**5**)) and $(\text{PC}_{\text{sp}^3}\text{P}^{\text{i-Pr}})\text{Ni}(\text{OH})$, **6**.

Results and Discussion

Preparation of $(\text{PC}_{\text{sp}^3}\text{P}^{\text{i-Pr}})\text{Ni}(\text{BF}_4)$, **1.** Reacting the complexes $(\text{PC}_{\text{sp}^3}\text{P}^{\text{i-Pr}})\text{NiR}$ ($\text{R} = \text{Me}, \text{Ph}, \text{C}\equiv\text{CMe}$) with $\text{HCl}\cdot\text{Et}_2\text{O}$ produces the previously reported^{10b} Ni-Cl derivative (Scheme 1). We reasoned that the analogous protonolysis reaction with Brønsted acids HX wherein X is a weakly coordinating conjugate base should generate either the coordinatively and electronically unsaturated cation $[(\text{PC}_{\text{sp}^3}\text{P}^{\text{i-Pr}})\text{Ni}][\text{X}]$ or $[(\text{PC}_{\text{sp}^3}\text{P}^{\text{i-Pr}})\text{Ni-X}]$, both of which should

be highly reactive species. Monitoring the reaction of $(\text{PC}_{\text{sp}^3}\text{P}^{\text{i-Pr}})\text{Ni}(\text{C}\equiv\text{CMe})$ with 1 equiv of $\text{HBF}_4\cdot\text{Et}_2\text{O}$ by $^{31}\text{P}\{^1\text{H}\}$ NMR spectroscopy showed that all the starting material was instantaneously converted into a new species that displayed a broad resonance at 63.5 ppm. An identical spectrum was obtained from the reaction of $(\text{PC}_{\text{sp}^3}\text{P}^{\text{i-Pr}})\text{NiBr}$ with 1 equiv of AgBF_4 (Scheme 1).

The facile protonation of $(\text{PC}_{\text{sp}^3}\text{P}^{\text{i-Pr}})\text{Ni}(\text{C}\equiv\text{CMe})$ and access to the corresponding Ni-Me and Ni-Ph analogues prompted us to probe the reactivities of the Ni-R moieties in these complexes as a function of the different hybridizations of the nickellated carbon atom ($\text{C}_{\text{sp}}, \text{C}_{\text{sp}^2}, \text{C}_{\text{sp}^3}$). Monitoring the reactions of $(\text{PC}_{\text{sp}^3}\text{P}^{\text{i-Pr}})\text{NiR}$ with $\text{HBF}_4\cdot\text{Et}_2\text{O}$ by $^{31}\text{P}\{^1\text{H}\}$ NMR spectroscopy showed the formation of the product obtained from the reaction of the $\text{Ni-C}\equiv\text{CMe}$ derivative (Scheme 1). Competition experiments were performed to assess the relative rates of protonation¹⁴ of the Ni-R derivatives. Thus, 3 equiv of $\text{HBF}_4\cdot\text{Et}_2\text{O}$ or $\text{HCl}\cdot\text{Et}_2\text{O}$ were added, 1 equiv at a time, to two C_6D_6 solutions containing 1 equiv of each of the three complexes $(\text{PC}_{\text{sp}^3}\text{P}^{\text{i-Pr}})\text{NiR}$ ($\text{R} = \text{Me}, \text{Ph}, \text{C}\equiv\text{CMe}$) and $^{31}\text{P}\{^1\text{H}\}$ NMR spectra were recorded between successive additions. The results revealed that the relative ease of protonation of the three complexes by either acid follows the decreasing order $\text{Ni-Me} > \text{Ni-C}\equiv\text{CMe} > \text{Ni-Ph}$. It is noteworthy that the kinetic reactivities of these Ni-C bonds, as defined by the relative ease of protonation of the Ni-R moiety, follows the order $\text{Ni-C}_{\text{sp}^3} > \text{Ni-C}_{\text{sp}} > \text{Ni-C}_{\text{sp}^2}$, whereas the thermodynamic strength of the Ni-C bond, as reflected in the respective Ni-C bond lengths for these compounds,^{10b} follows the order $\text{Ni-C}_{\text{sp}} > \text{Ni-C}_{\text{sp}^2} > \text{Ni-C}_{\text{sp}^3}$.¹⁵

Characterization of $(\text{PC}_{\text{sp}^3}\text{P}^{\text{i-Pr}})\text{Ni}(\text{BF}_4)$, **1.** All attempts to characterize the new complex **1** by elemental analysis or X-ray diffraction studies gave results consistent with the water-coordinated adduct $[(\text{PC}_{\text{sp}^3}\text{P}^{\text{i-Pr}})\text{Ni}(\text{H}_2\text{O})][\text{BF}_4]$, **2** (vide infra); nevertheless, a number of NMR spectral features and comparisons to literature precedents (Table 1) indicate that **1** possesses the structure illustrated in Scheme 1 wherein the Ni-BF_4 moiety involves fluxional Ni-F-BF_3 interactions. To begin with, the $^{31}\text{P}\{^1\text{H}\}$ and $^{13}\text{C}\{^1\text{H}\}$ NMR spectra of **1** are very similar to the corresponding spectra for $(\text{PC}_{\text{sp}^3}\text{P}^{\text{i-Pr}})\text{NiX}$ ($\text{X} = \text{Cl}, \text{Br}$; Table 1), which implies that the overall structure of **1** must be quite similar to those of the completely characterized halide derivatives. On the other

(9) (a) Castonguay, A.; Sui-Seng, C.; Zargarian, D.; Beauchamp, A. L. *Organometallics* **2006**, *25*, 602. (b) Sui-Seng, C.; Castonguay, A.; Chen, Y.; Gareau, D.; Groux, L. F.; Zargarian, D. *Top. Catal.* **2006**, *37*, 81.

(10) (a) Castonguay, A.; Beauchamp, A. L.; Zargarian, D. *Acta Crystallogr.* **2007**, *E63*, m196. (b) Castonguay, A.; Zargarian, D.; Beauchamp, A. L. *Organometallics* **2008**, *27*, 5723.

(11) Significant reactivity differences also exist between $\text{PC}_{\text{sp}^2}\text{P}$ - and $\text{NC}_{\text{sp}^2}\text{N-Ni}$ complexes. For a lead reference on the reactivities of $\text{NC}_{\text{sp}^2}\text{N-Ni}$ complexes see van Koten's review in ref 2a.

(12) Similarly, we have shown that oxidation of the phosphinite analogues of our $\text{PC}_{\text{sp}^3}\text{P}^{\text{i-Pr}}\text{-Ni}$ complexes, $(\text{POC}_{\text{sp}^2}\text{OP}^{\text{i-Pr}})\text{NiX}$ ($\text{X} = \text{Cl}, \text{Br}$), give isolable Ni^{III} complexes, whereas Ni^{III} complexes based on the ligand $\text{POC}_{\text{sp}^2}\text{OP}^{\text{i-Pr}}$ can be generated electrochemically but do not appear to be isolable. For the chemistry of $(\text{POC}_{\text{sp}^2}\text{OP}^{\text{i-Pr}})\text{-Ni}$ complexes see: (a) Pandarus, V.; Zargarian, D. *Chem. Commun.* **2007**, 978. (b) Pandarus, V.; Zargarian, D. *Organometallics* **2007**, *26*, 4321.

(13) It is worth noting that van Koten's group has reported the first examples of Ni^{III} pincer complexes based on the $\text{NC}_{\text{sp}^2}\text{N}$ -type ligands: Grove, D. M.; van Koten, G.; Zoet, R. *J. Am. Chem. Soc.* **1983**, *105*, 1379.

(14) We define the observed rate as that of the overall reaction of the Ni-R species with $\text{R}'\text{-H}$ to give $\text{Ni-R}' + \text{R-H}$.

(15) We offer the following analysis in response to a reviewer who asked that we consider the relative strengths of the resulting C-H bonds when comparing relative rates of the "protonation" reactions. In the case of $\text{LNi-CC-Me} + \text{Ph-CC-H}$, the Ni-C and the C-H bonds are both stronger in the products (Ni-CC-Ph and Me-CC-H , respectively); in addition, propene is volatile which should drive the equilibrium to the right. Therefore, this reaction should be favorable, as was observed. In contrast, the reactions of LNi-Me and LNi-Ph with Ph-CC-H lead to products having weaker C-H bonds (methane and benzene), a factor that should not favor these reactions. In the case of $\text{LNi-Me} + \text{Ph-CC-H}$, the resulting Ni-C bond is much stronger ($\text{sp} > \text{sp}^3$) and methane is a volatile gas, two factors that drive the reaction. On the other hand, in the case of $\text{LNi-Ph} + \text{Ph-CC-H}$, the resulting Ni-C bond is stronger, but to a lesser extent; moreover, M-Ph are generally less reactive (i.e., kinetically more stable) than M-CC-R . These two factors should combine to retard the "protonation" of the thermodynamically weaker Ni-Ph bond.

Table 1. Comparison of Room Temperature NMR Data for Complexes $(\text{PC}_{\text{sp}^3\text{P}^i\text{Pr}})\text{Ni}(\text{BF}_4)$ (**1**), $[(\text{PC}_{\text{sp}^3\text{P}^i\text{Pr}})\text{Ni}(\text{OH}_2)][\text{BF}_4]$ (**2**), and $(\text{PC}_{\text{sp}^3\text{P}^i\text{Pr}})\text{NiX}$ (X = Cl, Br, I)^a

	Assignment	$(\text{PC}_{\text{sp}^3\text{P}^i\text{Pr}})\text{NiX}$ (C_6D_6)					
		1		2	X = Cl	X = Br	X = I
		(C_6D_6)	(CDCl_3)	(CDCl_3)			
$^{31}\text{P}\{^1\text{H}\}$		63.5	64.0	66.5	66.5	67.4	70.5
$^{19}\text{F}\{^1\text{H}\}$		-179		-145 ^b	---	---	---
$^{13}\text{C}\{^1\text{H}\}$	CH(CH ₃) ₂	17.5, 18.4, 19.3, 19.4	17.7, 18.6, 19.3, 19.4	17.7, 18.6, 19.4, 19.5	17.6, 18.6, 19.3, 19.7	17.6, 18.6, 19.4, 19.9	17.7, 18.7, 19.5, 20.4
	α	18.6	18.7	19.3	21.8	22.1	22.7
	CH(CH ₃) ₂	22.7, 24.5	22.6, 24.4	22.5, 24.4	22.9, 25.0	23.4, 25.5	24.4, 26.4
	β	38.7	38.5	38.2	39.0	38.9	38.8
	γ	--- ^c	--- ^c	43.3	48.7	52.3	58.0

^a Data for the Ni–halide derivatives are taken from ref 10b. ^b This spectrum was recorded in C_6D_6 . ^c A DEPT 90 NMR experiment has hinted that these signals appear at about 38.7 (C_6D_6) and 38.5 ppm (CDCl_3) but are obscured in the $^{13}\text{C}\{^1\text{H}\}$ NMR spectrum by the signal due to the β -carbons.

hand, the $^{19}\text{F}\{^1\text{H}\}$ NMR spectrum of **1** supports the proposal that BF_4^- has bonding interactions with the Ni center: a very broad ^{19}F resonance was observed at -179 ppm (in C_6D_6), significantly upfield of the corresponding signals displayed by $\text{HBF}_4 \cdot \text{Et}_2\text{O}$ (-153 ppm in C_6D_6) and the closely related complexes $[(\text{PC}_{\text{sp}^3\text{P}^i\text{Pr}})\text{NiL}][\text{BF}_4]$ in which BF_4^- is a non-coordinating anion (e.g., -145 to -152 ppm, vide infra). In a similar fashion, the PCN-type pincer complexes $\{2\text{-(CH}_2\text{P}(t\text{-Bu})_2)\text{6-(CH}_2\text{NEt}_2)\text{C}_6\text{H}_3\}\text{Rh}(\text{BF}_4)(\text{CH}_3)$ ^{16a} and $\{2\text{-(CH}_2\text{P}(t\text{-Bu})_2)\text{6-((CH}_2)_n\text{NR}_2)\text{C}_6\text{H}_3\}\text{Pt}(\text{BF}_4)$ ($n = 1$: R = Et; $n = 2$: R = Me)^{16b} show $^{19}\text{F}\{^1\text{H}\}$ signals at about -164 (2,5-dimethyltetrahydrofuran) and -162 (CD_2Cl_2) ppm for the Rh and Pt complexes, respectively, significantly upfield of the signal for free BF_4^- (ca. -151 ppm, 2,5-dimethyltetrahydrofuran or CD_2Cl_2).¹⁶

Comparisons of variable temperature NMR data obtained for **1** and reported for related complexes provided additional support for the existence of fluxional Ni–F– BF_3 interactions. For instance, observation of two ^{31}P signals coalescing at about -30 °C for the closely related PCP complex $(\text{PC}_{\text{sp}^3\text{P}^i\text{Pr}})\text{Pd}(\text{BF}_4)$ has been attributed to a rapid exchange between BF_4^- and CD_2Cl_2 .¹⁷ Our own variable temperature NMR experiments showed that the broad ^{31}P signal observed at room temperature for **1** splits into two sharp singlets at -25 °C (ca. 65 and 63 ppm, ratio 1:1.9, toluene- d_8), which coalesce at ~ 10 °C into a broad resonance at ~ 64 ppm; the latter then sharpens as the temperature is increased. These observations imply a fairly slow exchange between coordinated and free BF_4^- , but the data obtained was not sufficiently unambiguous to establish whether solvent coordination takes place. On the other hand, repeating the low-temperature experiment showed a different ratio of the ^{31}P signals, the peak at 65 ppm being much less intense. This observation, combined with the fact that the ^{31}P NMR signal for the independently prepared aquo complex $[(\text{PCPNi}(\text{OH}_2))]$ (**2**) is in the same region (ca. 66 ppm, vide infra), suggests the possible coordination of some residual water that would be present in variable amounts in the $\text{HBF}_4/\text{Et}_2\text{O}$ solution

used to generate **1** from $(\text{PCP})\text{NiC}\equiv\text{CMe}$. This hypothesis is also consistent with the results of low temperature $^{19}\text{F}\{^1\text{H}\}$ NMR studies that showed two peaks of similar ratios as seen in the ^{31}P NMR spectra: the major peak appears in the region generally known for coordinated BF_4^- anions (s, -179 ppm), while the minor one is found in the region for non-coordinated BF_4^- anions (br s, -148 ppm), very close to the corresponding ^{19}F NMR signal observed for the independently observed aquo complex **2**.

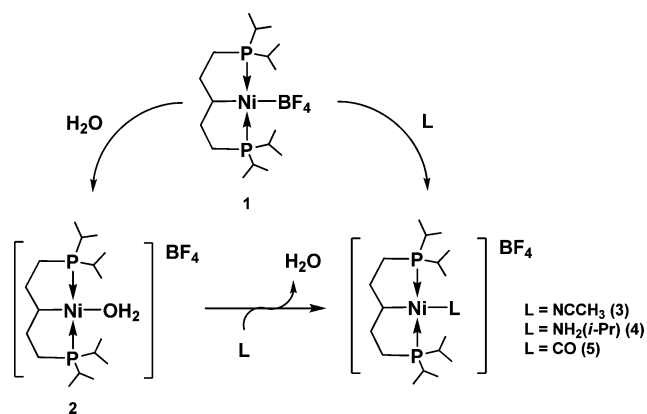
The issue of $\text{BF}_4^-/\text{solvent}$ exchange has been discussed in a report on the Rh– BF_4^- complex $\{2\text{-(CH}_2\text{P}(t\text{-Bu})_2)\text{6-(CH}_2\text{NEt}_2)\text{C}_6\text{H}_3\}\text{Rh}(\text{BF}_4)(\text{CH}_3)$.^{16b} Thus, the low-temperature $^{19}\text{F}\{^1\text{H}\}$ NMR experiments of this compound supported $\text{BF}_4^-/\text{solvent}$ exchange in a coordinating solvent such as THF, whereas the ^{19}F signal remained unchanged when the experiments were performed in a non-coordinating solvent such as 2,6-dimethyltetrahydrofuran. On the other hand, spin-saturation experiments carried out on this compound in the same non-coordinating solvent supported the exchange between the coordinated and free BF_4^- , implying that solvent coordination might not be required for this exchange process. In the case of our complexes, we have considered the possibility that the observed exchange process involves BF_4^-/N_2 exchange as opposed to solvent binding, but this was ruled out because identical $^{31}\text{P}\{^1\text{H}\}$ NMR spectra were obtained for samples of **1** prepared from the reaction of $(\text{PC}_{\text{sp}^3\text{P}^i\text{Pr}})\text{NiBr}$ with AgBF_4 under a nitrogen or argon atmosphere. Also, we have ruled out the possibility that the propyne gas generated from this reaction coordinates to Ni based on the observation that adding many equivalents of PhCCH to the tube did not alter the $^{31}\text{P}\{^1\text{H}\}$ NMR chemical shift of the $(\text{PCP})\text{NiBF}_4$ species, implying that alkyne coordination is not competitive.

We conclude on the basis of the above observations and literature comparisons that complex **1** is more appropriately described as the charge-neutral species $(\text{PC}_{\text{sp}^3\text{P}^i\text{Pr}})\text{Ni}(\text{BF}_4)$ (Scheme 1) involving rapidly fluxional Ni–F– BF_3 interactions, as opposed to the charge-separated species $[(\text{PC}_{\text{sp}^3\text{P}^i\text{Pr}})\text{Ni}][\text{BF}_4]$.¹⁸ The proposed structure for **1** is also consistent with the empirical correlation we have noted in $(\text{PC}_{\text{sp}^3\text{P}^i\text{Pr}})\text{NiX}$ complexes between the ^{31}P chemical shift values and nature of X (size, electronegativity, polarizability, and

(16) (a) Gandelman, M.; Konstantinovski, L.; Rozenberg, H.; Milstein, D. *Chem. Eur. J.* **2003**, *9*, 2595. (b) Poverenov, E.; Gandelman, M.; Shimon, L. J. W.; Rozenberg, H.; Ben-David, Y.; Milstein, D. *Organometallics* **2005**, *24*, 1082.

(17) Seligson, A. L.; Troglor, W. C. *Organometallics* **1993**, *12*, 738.

Scheme 2



π -donor strength of the atom bonded to Ni): F-BF₃ (~64 ppm) < OH₂ ~ Cl (66.5 ppm) < Br (67.4 ppm) < I (70.5 ppm).

Preparation of Cationic Adducts from 1. Reaction of **1** with 1 equiv of water in C₆D₆ or CDCl₃ led to a color change from orange to yellow, and NMR spectra indicated the clean conversion of **1** to the new aquo species [(PC_{sp3}-P^{i-Pr})Ni(OH₂)](BF₄)₂, **2** (Table 1, Scheme 2). Thus, the ³¹P{¹H} NMR showed a singlet at 66.5 ppm, ~2 ppm downfield of the corresponding signal for **1**; similar downfield displacements were also observed for the ¹³C signals corresponding to α - and γ -carbons. It is noteworthy that the signal for γ -C was a triplet (²J_{PC} = 7.2 Hz) and the ¹⁹F{¹H} NMR spectrum of **2** showed a broad signal at -145 ppm (Table 1), which is characteristic of a non-coordinated BF₄⁻ counterion (vide supra). The ¹H NMR spectrum of **2** did not show a signal for the coordinated water molecule, but addition of a few equivalents of water to an NMR sample¹⁹ gave rise to a signal at 5.29 ppm (C₆D₆) whose intensity grew with successive additions of water. The presence of a water molecule in solid samples of **2** has been confirmed by the combustion data, as well as by the IR spectrum (KBr pellets) that showed a strong band at 3444 cm⁻¹ assigned to ν (OH).

Single crystals of **2** were easily grown, and its solid-state structure was established from an X-ray diffraction study. The Oak Ridge Thermal Ellipsoid Plot (ORTEP) view is shown in Figure 1, crystal data and collection details are listed in Table 2, and selected bond distances and angles are given in Table 3. The solid-state structure of **2** consists of a square planar complex featuring a Ni-OH₂ moiety. Relative to the neutral complex (PC_{sp3}P^{i-Pr})NiBr,^{10b} the Ni-C γ distance is nearly unchanged (~1.97 Å vs ~1.98 Å), but the Ni-P bond distances are longer in **2** (~2.21 Å vs ~2.18 Å). The Ni-O bond distance observed in **2** (~2.00 Å) is shorter than the mean of all the Ni-O bond lengths reported in the literature for monocationic water-coordinated

complexes (2.087(3) Å).²⁰ It should be noted, however, that most aquo complexes of Ni are penta- or hexa-coordinated species that would be expected to have somewhat longer Ni-ligand bond lengths. The proximity of the counterion to the water molecule suggests the presence of hydrogen bonds

Three other cationic adducts [(PC_{sp3}P^{i-Pr})Ni(L)](BF₄) were prepared from the reaction of **1** with CH₃CN (**3**), *i*-PrNH₂ (**4**) or CO (**5**); these new complexes were also obtained by the reaction of the aquo adduct **2** with 1 equiv of CH₃CN or NH₂(*i*-Pr), or with 1 atm of CO (Scheme 2). The conversion of **2** to **3** was indicated by the emergence of a new ³¹P signal at 76.7 ppm. The presence of a coordinated acetonitrile in **3** was confirmed by the observation of a new ¹H signal at 0.63 ppm and two ¹³C signals at δ 3.24 (CH₃CN) and 132.59 (CH₃CN). The change in the ³¹P{¹H} spectrum was nearly imperceptible during the reaction of **2** with *i*-PrNH₂ (singlet shifting from 65.8 to 65.5 ppm), but the formation of **4** was inferred from the emergence of two new ¹³C signals for the coordinated *i*-PrNH₂, a singlet at ~25 ppm for CH₃ (vs a singlet at ~26 ppm in free *i*-PrNH₂), and a triplet at ~50 ppm for CH (³J_{PC} = 3.8 Hz, vs a singlet at ~43 ppm in free *i*-PrNH₂). In contrast, formation of the CO adduct **5** caused significant downfield shifts of the ³¹P signal (>20 ppm) and the ¹³C resonance attributed to γ -C (>30 ppm). Curiously, the signal for γ -C is a singlet, not the anticipated triplet, but we were able to confirm this assignment based on a DEPT135 experiment.²¹ Finally, the corresponding ¹³C resonance for CO was not detected, but the observation of a ν (CO) band in the solid-state IR spectrum indicated a significant Ni-CO π -donation (2040 cm⁻¹ for **5** vs 2143 cm⁻¹ for free CO).²²

X-ray analyses allowed us to study the solid-state structures of complexes **3**–**5**. Crystal data and collection details are listed in Table 2, and selected bond distances and angles are given in Table 3. As seen in the ORTEP diagrams (Figure 2), the Ni center maintains a square-planar geometry, and the Ni-P bond distances (~2.20–2.23 Å) are quite similar to the corresponding distances in the aquo precursor **2**. The Ni-C bond lengths are also similar in **2**–**4** (~1.97–1.99 Å) and in **3**–**5** (~1.98–2.00 Å), the one in **5** (~2.00 Å) being slightly longer than the one in **2** or **3** (~1.97–1.98 Å), which can be explained by the greater trans influence of CO compared to water or amines. The Ni-N (1.897(2) Å) and the N≡C (1.141(3) Å) bond distances in **3** are similar to the corresponding bond lengths in the analogous complex [(PC_{sp3}P^{t-Bu})Ni(N≡CCH₃)](BPh₄)₂,^{9a} which probably implies that the Ni-NCCH₃ bond is dominated by N→Ni σ -donation. The Ni-N bond distance in **4** (2.0261(18) Å) is significantly shorter than the mean of all the Ni-N bond lengths of coordinated primary amines reported in the literature for Ni^{II}

(18) A reviewer of our manuscript has pointed out that this conclusion might be reasonable only in non-polar solvents such as toluene-d₈ in which the NMR experiments were performed. We agree with this stipulation.

(19) The sample is a suspension because complex **2** is only partially soluble in C₆D₆.

(20) Cambridge Structural Database search (Version 5.28 with updates up to November 2006; Allen, F. H. *Acta Crystallogr.* **2002**, *B58*, 380).

(21) It is interesting to note that there seems to be a correlation between the chemical shifts of the γ -C and the ³¹P signals for PC_{sp3}P^{i-Pr}-Ni complexes. See graph included in the Supporting Information section.

(22) Crabtree, R. H. *The Organometallic Chemistry of the Transition Metals*, 4th ed.; Wiley: Hoboken, NJ, 2005.

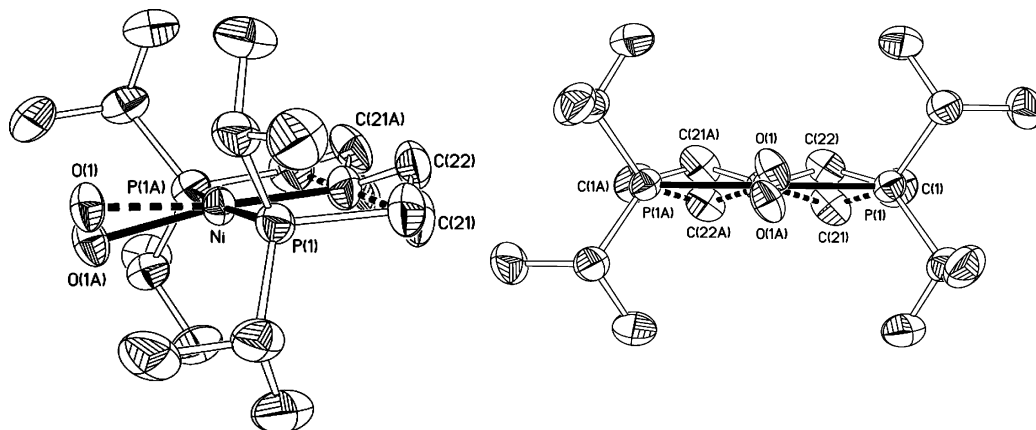


Figure 1. Side and front views of the ORTEP diagram for complex **2**. Thermal ellipsoids are shown at the 30% probability level. The hydrogens as well as the BF_4^- counterion are omitted for clarity. The β carbons as well as the Ni-coordinated oxygen atom were found to occupy two positions (50:50).

Table 2. Data Collection and Refinement Parameters for Complexes and **2–6**

	2	3	4	5	6
chemical formula	$\text{C}_{17}\text{H}_{39}\text{NiP}_2\text{F}_4\text{OB}$	$\text{C}_{19}\text{H}_{40}\text{NiP}_2\text{F}_4\text{NB}$	$\text{C}_{20}\text{H}_{46}\text{NiP}_2\text{F}_4\text{NB}$	$\text{C}_{18}\text{H}_{37}\text{NiP}_2\text{F}_4\text{OB}$	$\text{C}_{17}\text{H}_{38}\text{NiP}_2\text{O}$
Fw	466.94	489.98	508.04	476.94	379.12
T (K)	220(2)	150(2)	150(2)	150(2)	100(2)
wavelength (\AA)	1.54178	1.54178	1.54178	1.54178	1.54178
space group	$P4_22_12$	$P2_12_12_1$	$P\bar{1}$	$P2/c$	$P2_1/n$
a (\AA)	14.6664(9)	11.3041(5)	8.7544(4)	13.8041(6)	10.3090(4)
b (\AA)	14.6664(9)	14.7679(7)	11.5109(5)	8.3146(4)	17.0475(6)
c (\AA)	11.0426(14)	15.4458(8)	13.6825(5)	20.7105(8)	11.9074(4)
α (deg)	90	90	72.912(2)	90	90
β (deg)	90	90	87.199(2)	100.103(2)	105.6150(10)
γ (deg)	90	90	83.003(2)	90	90
Z	4	4	2	4	4
V (\AA^3)	2375.3(4)	2578.5(2)	1307.99(10)	2340.20(18)	2015.40(13)
ρ_{calcd} (g cm^{-3})	1.306	1.262	1.290	1.354	1.249
μ (cm^{-1})	27.64	25.54	25.31	28.20	28.53
θ range (deg)	4.26–72.01	4.14–60.44	3.38–71.80	3.25–73.15	4.65–67.06
$R1^a$ [$I > 2\sigma(I)$]	0.0477	0.0343	0.0441	0.0392	0.0309
$wR2^b$ [$I > 2\sigma(I)$]	0.1300	0.0910	0.1192	0.1099	0.0850
$R1$ [all data]	0.0493	0.0354	0.0484	0.0467	0.0322
$wR2$ [all data]	0.1316	0.0919	0.1222	0.1142	0.0859
GOF	1.040	1.052	0.957	1.096	1.049

^a $R1 = \sum ||F_o| - |F_c|| / \sum |F_o|$. ^b $wR2 = \{\sum [w(F_o^2 - F_c^2)^2] / \sum w(F_o^2)^2\}^{1/2}$.

Table 3. Selected Bond Distances (\AA) and Angles (deg) for Complexes **2–6**

	2 (X = O)	3 (X = N)	4 (X = N)	5 (X = C)	6 (X = O)
Ni–C(3)	1.965(8)	1.981(3)	1.989(2)	2.000(2)	1.9856(16)
Ni–P(1)	2.2086(18)	2.1971(7)	2.2305(6)	2.2010(6)	2.1687(5)
Ni–P(2)	2.2086(18) ^a	2.2016(7)	2.2014(6)	2.2013(6)	2.1635(5)
Ni–X	1.997(8)	1.897(2)	2.0261(18)	1.780(2)	1.8793(14)
C(3)–Ni–X	171.4(7)	176.96(12)	173.04(11)	177.36(10)	173.51(7)
P(1)–Ni–P(2)	171.20(11) ^a	169.99(3)	168.54(3)	169.25(3)	170.26(2)
P(1)–Ni–X	95.0(8)	93.89(7)	97.64(6)	94.77(7)	98.38(5)
P(2)–Ni–X	95.0(8) ^a	96.08(7)	93.80(6)	95.74(7)	90.93(5)
P(1)–Ni–C(3)	85.6(5)	84.97(8)	84.82(6)	84.54(7)	85.58(5)
P(2)–Ni–C(3)	85.6(5) ^a	85.11(8)	83.88(6)	85.07(7)	84.90(5)

^a Symmetry transformation used to generate equivalent atoms: $y, x, -z + 2$.

monocationic species (2.074(3) \AA).²⁰ It should be noted, however, that most amino complexes of Ni are penta- or hexa-coordinated species that would be expected to have somewhat longer Ni–ligand bond lengths. The hydrogen atoms of the NH_2 moiety were positioned from residual peaks in the difference Fourier map, and the N–H bond distances (0.86(3) \AA) were found to be comparable to other N–H bond length values found in the literature.²⁰ The C–O bond distance in **5** was found to be 1.139(3) \AA , which is similar to the one found in free CO (~ 1.128 \AA).²³

Deprotonation of 2. NMR monitoring of the reaction of **2** with 1 equiv of $\text{KN}(\text{SiMe}_3)_2$ showed the disappearance of the $^31\text{P}\{^1\text{H}\}$ singlet at 65.8 ppm (C_6D_6)¹⁹ and the emergence of a signal at 62.8 ppm along with variable amounts of side-products (<5%) at 66.2 ppm and 60.3 ppm. These minor species have not been characterized, but the major product was identified as the hydroxo complex **6** (Scheme 3). The ^1H NMR spectrum of **6** showed a triplet signal at -3.05

(23) Cotton, F. A.; Wilkinson, G. *Advanced Inorganic Chemistry*, 4th ed.; Wiley: New York, 1980.

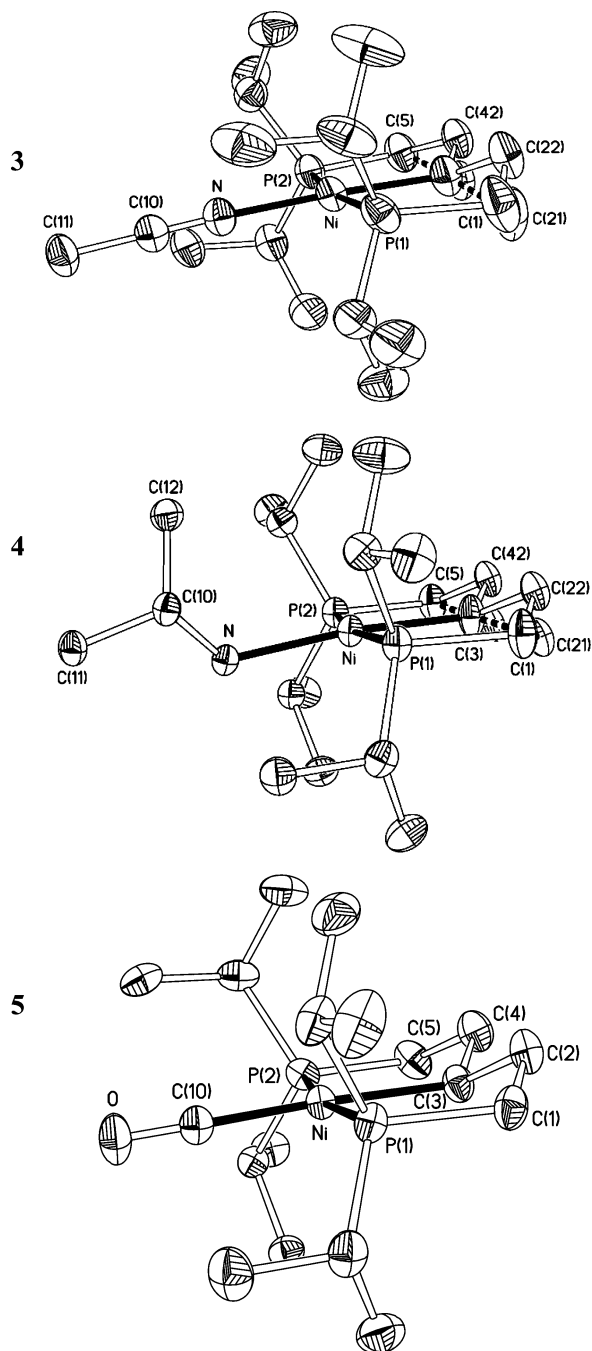
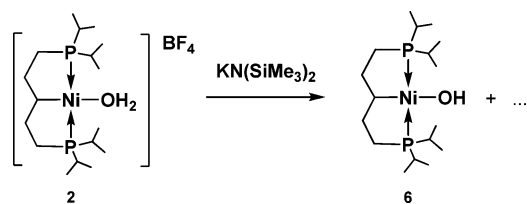


Figure 2. ORTEP diagrams for complex **3**, **4**, and **5**. Thermal ellipsoids are shown at the 30% probability level. The hydrogens as well as the BF_4^- counterions are omitted for clarity. Some disorder was taken into account for the β carbons of **3** (40:60) and **4** (30:70), and for half of the BF_4^- moieties of the molecular structure of **5** (50:50).

Scheme 3



ppm ($^3J_{\text{HP}} = 6.1$ Hz), assigned to the OH moiety, whereas the $^{19}\text{F}\{^1\text{H}\}$ NMR spectrum showed no signals at all. A $\text{PC}_{\text{sp}^2}\text{P}$ analogue of **6**, $[\{(i\text{-Pr}_2\text{PCH}_2)_2\text{C}_6\text{H}_3\}\text{NiOH}]$, has been

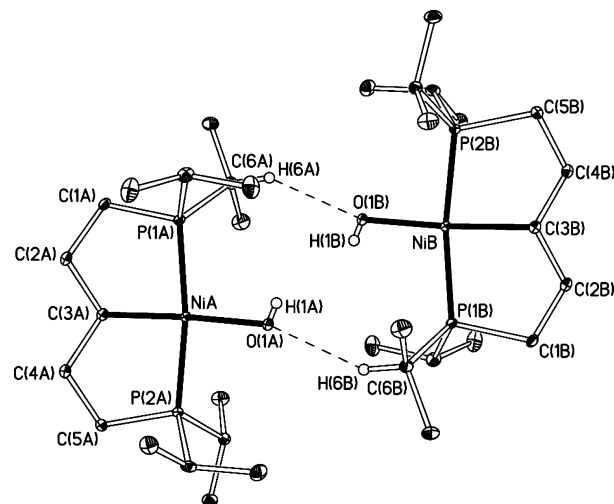


Figure 3. ORTEP diagram for complex **6**. Thermal ellipsoids are shown at the 30% probability level. The hydrogens of the PCP ligand which are not involved in the weak intermolecular interaction are omitted for clarity.

reported recently,^{8f} and the NMR data for this complex are similar to those of **6**, in particular the ^1H NMR triplet attributed to its OH moiety (-2.52 ppm, $^3J_{\text{HP}} = 6.4$ Hz).

Single crystals of **6** were grown, and its solid-state structure was confirmed by an X-ray analysis. The ORTEP view is shown in Figure 3, the crystal data and collection details are listed in Table 2, and selected bond distances and angles are given in Table 3. In the molecular structure of **6**, the geometry around the nickel center is square planar, and the PCP-Ni bond distances are in the same range as those observed for the previously reported neutral complexes $(\text{PC}_{\text{sp}^3}\text{P}^{i\text{-Pr}})\text{NiR}$ bearing the same ligand ($\text{R} = \text{Br}, \text{Me}, \text{Ph}, \text{C}\equiv\text{CMe}$).^{10b} Curiously, there seems to be a weak hydrogen-bonding type interaction between the oxygen of one molecule of **6** and an $i\text{-Pr}$ proton of the other molecule; a similar situation was observed in the structure of $[\{(i\text{-Pr}_2\text{PCH}_2)_2\text{C}_6\text{H}_3\}\text{Ni}(\text{OH})]$.^{8f} The Ni-O bond distance observed in the latter $\text{PC}_{\text{sp}^2}\text{P}$ analogue is slightly shorter than the corresponding distances found in **6** and $\text{cis-}\{(i\text{-Pr}_2\text{P}(\text{CH}_2)_2\text{P}(i\text{-Pr})_2)\text{Ni}(\text{OH})(\text{Me})\}$ ²⁴ (~ 1.86 vs ~ 1.88 Å).

Conclusion

It has been shown that $(\text{PC}_{\text{sp}^3}\text{P}^{i\text{-Pr}})\text{Ni}(\text{BF}_4)$ involves fluxional Ni-F-BF_3 interactions. This species can be used to prepare cationic adducts with relatively weak nucleophiles such as water, and it is hoped that the lability of the BF_4^- moiety will prove useful in catalytic applications requiring the coordination of weakly coordinating substrates. The new hydroxo complex $(\text{PC}_{\text{sp}^3}\text{P}^{i\text{-Pr}})\text{Ni}(\text{OH})$ was also prepared from its aquo precursor, and efforts are underway to study its reactivity in insertion reactions.

Experimental Section

General Comments. All manipulations were carried out under a nitrogen atmosphere using standard Schlenk techniques and/or in nitrogen-filled glovebox, except where noted. Solvents were

(24) Cámpora, J.; Matas, I.; Palma, P.; Graiff, C.; Tiripicchio, A. *Organometallics* **2005**, *24*, 2827.

purified by distillation from appropriate drying agents before use. All reagents were used as received from commercial vendors while precursors have been prepared according to a previously reported article.^{10b} All the NMR spectra were recorded at ambient temperature on Bruker instruments: AV400 (¹H, ¹H{³¹P}), AV300 (³¹P{¹H}, ¹⁹F{¹H}) and ARX400 (¹³C{¹H}). The ¹H and ¹³C{¹H} NMR spectra were referenced to solvent resonances while the ³¹P{¹H} and ¹⁹F{¹H} NMR spectra were respectively referenced to an external 85% H₃PO₄ and C₆H₅CF₃ samples (0 ppm). The IR spectra were recorded on a Perkin-Elmer 1750 FTIR (4000–450 cm⁻¹) with samples prepared as KBr pellets. The ^vJ term used refers to the apparent coupling constant of the virtual triplets. The elemental analyses were performed by the Laboratoire d'Analyse Élémentaire (Université de Montréal).

[(*i*-Pr)₂PCH₂CH₂]₂CHNi(BF₄) (1). Method A. HBF₄ (5 μL of a 54 wt % solution in Et₂O, 0.04 mmol) was added to an NMR tube containing a solution of (PC_{sp₃P^{i-Pr}})NiC≡CMe (0.015 g, 0.04 mmol) in C₆D₆ (0.6 mL). The color of the solution changed from yellow to dark orange instantaneously.

Method B. To a solution of (PC_{sp₃P^{i-Pr}})NiBr (0.100 g, 0.23 mmol) in C₆D₆ (0.6 mL) was added AgBF₄ (0.053 g, 0.27 mmol), and the suspension was heated to 80 °C for 1 h. The reaction mixture was then filtered into an NMR tube. In both cases, the orange solution obtained was analyzed by NMR spectroscopy, and the resultant product was identified as complex **1**. ¹H NMR (C₆D₆): 0.30–1.50 (m, CH₂CH₂P, NiCH, 9H), 0.87 (dvt, ^vJ_{PH} ~ ^vJ_{HH} = 6.1–7.0 Hz, CH(CH₃)₂, 6H), 1.05 (dvt, ^vJ_{PH} ~ ^vJ_{HH} = 6.8–7.0 Hz, CH(CH₃)₂, 6H), 1.38 (dvt, ^vJ_{PH} ~ ^vJ_{HH} = 7.4–7.8 Hz, CH(CH₃)₂, 6H), 1.45 (dvt, ^vJ_{PH} ~ ^vJ_{HH} = 8.1–8.3 Hz, CH(CH₃)₂, 6H), 1.97 (m, CH(CH₃)₂, 2H), 2.11 (m, CH(CH₃)₂, 2H). ¹³C{¹H} NMR (C₆D₆): 17.46 (s, CH(CH₃)₂, 2C), 18.43 (s, CH(CH₃)₂, 2C), 18.56 (partially hidden vt, ^vJ_{PC} = 11.4 Hz, CH₂P, 2C), 19.27 (s, CH(CH₃)₂, 2C), 19.44 (s, CH(CH₃)₂, 2C), 22.70 (vt, ^vJ_{PC} = 9.5 Hz, CH(CH₃)₂, 2C), 24.46 (vt, ^vJ_{PC} = 9.5 Hz, CH(CH₃)₂, 2C), 38.68 (hidden t, ²J_{PC} = 9.3 Hz, NiC, 1C), 38.72 (vt, ^vJ_{PC} = 8.5 Hz, CH₂CH₂P, 2C). ³¹P{¹H} NMR (C₆D₆): 63.5 (s). ³¹P{¹H} NMR (CDCl₃): 64.0 (s). ¹⁹F{¹H} NMR (C₆D₆): -179 (br s).

[(*i*-Pr)₂PCH₂CH₂]₂CHNi(OH₂)[BF₄] (2). Method A. To a solution of (PC_{sp₃P^{i-Pr}})NiC≡CMe (0.100 g, 0.25 mmol) in toluene (5 mL) was added HBF₄ (35 μL of a 54 wt % solution in Et₂O, 0.25 mmol). Water (0.2 mL) was added to the reaction mixture and complex **2** was obtained as a yellow powder after evaporation of the solvent to dryness (0.045 g, 39%).

Method B. A solution of (PC_{sp₃P^{i-Pr}})NiBr (0.120 g, 0.27 mmol) in toluene (3 mL) was added to a Schlenk tube containing AgBF₄ (0.063 g, 0.32 mmol), and the reaction mixture was heated to 80 °C for 1 h. The resultant suspension was filtered, and water (5 μL) was added to the filtrate. Complex **2** was obtained as a yellow powder after evaporation of the solvent to dryness (0.031 g, 24%). ¹H NMR (C₆D₆): 0.55–1.50 (m, CH₂CH₂P, NiCH, 9H), 0.92 (m, CH(CH₃)₂, 6H), 1.05 (m, CH(CH₃)₂, 6H), 1.39 (m, CH(CH₃)₂, 12H), 2.01 (m, CH(CH₃)₂, 2H), 2.13 (m, CH(CH₃)₂, 2H). ¹³C{¹H} NMR (CDCl₃): 17.65 (s, CH(CH₃)₂, 2C), 18.64 (s, CH(CH₃)₂, 2C), 19.26 (partially hidden vt, ^vJ_{PC} = 13.1 Hz, CH₂P, 2C), 19.39 (s, CH(CH₃)₂, 2C), 19.52 (s, CH(CH₃)₂, 2C), 22.48 (vt, ^vJ_{PC} = 10.3 Hz, CH(CH₃)₂, 2C), 24.42 (vt, ^vJ_{PC} = 9.3 Hz, CH(CH₃)₂, 2C), 38.24 (vt, ^vJ_{PC} = 9.0 Hz, CH₂CH₂P, 2C), 43.26 (t, ²J_{PC} = 7.2 Hz, NiC, 1C). ³¹P{¹H} NMR (CDCl₃): 66.5 (s). ³¹P{¹H} NMR (C₆D₆): 65.8 (s). ¹⁹F{¹H} NMR (C₆D₆): -145 (br s). IR (KBr): 3444 cm⁻¹, ν(O–H). Anal. Calcd for C₁₇H₃₉NiP₂O₄F₄: C, 43.73; H, 8.42. Found: C, 43.43; H, 8.47.

[(*i*-Pr)₂PCH₂CH₂]₂CHNi(NCCH₃)[BF₄] (3). Method A. To a solution of complex (PC_{sp₃P^{i-Pr}})NiC≡CMe (0.145 g, 0.36 mmol)

in toluene (2 mL) was added HBF₄ (55 μL of a 54 wt % solution in Et₂O, 0.40 mmol). CH₃CN was added to the reaction mixture, and complex **3** was obtained as a yellow-brown oily compound after evaporation of the solvent to dryness (0.071 g, 40%).

Method B. CH₃CN (2 μL, 0.03 mmol) was added to a NMR tube filled with a suspension¹⁹ of **2** (0.014 g, 0.03 mmol) in C₆D₆ (0.6 mL). A bleaching of the solution was instantaneously observed, and NMR spectroscopy confirmed that the substitution reaction took place. ¹H NMR (C₆D₆): 0.63 (s, CH₃CN, 3H), 0.80–1.70 (m, CH₂CH₂P, NiCH, 9H), 0.99 (m, CH(CH₃)₂, 12H), 1.23 (m, CH(CH₃)₂, 12H), 1.98 (m, CH(CH₃)₂, 2H), 2.19 (m, CH(CH₃)₂, 2H). ¹³C{¹H} NMR (C₆D₆): 3.24 (s, CH₃CN, 1C), 17.69 (s, CH(CH₃)₂, 2C), 18.75 (s, CH(CH₃)₂, 2C), 19.43 (s, CH(CH₃)₂, 2C), 19.52 (s, CH(CH₃)₂, 2C), 20.21 (vt, ^vJ_{PC} = 12.0 Hz, CH₂P, 2C), 22.98 (vt, ^vJ_{PC} = 10.2 Hz, CH(CH₃)₂, 2C), 25.16 (vt, ^vJ_{PC} = 9.9 Hz, CH(CH₃)₂, 2C), 38.55 (vt, ^vJ_{PC} = 8.6 Hz, CH₂CH₂P, 2C), 53.92 (t, ²J_{PC} = 5.8 Hz, NiC, 1C), 132.59 (s, CH₃CN, 1C). ³¹P{¹H} NMR (C₆D₆): 76.7 (s). ¹⁹F{¹H} NMR (C₆D₆): -152 (br s).

[(*i*-Pr)₂PCH₂CH₂]₂CHNi[NH₂(*i*-Pr)][BF₄] (4). Method A. To a solution of complex (PC_{sp₃P^{i-Pr}})NiC≡CMe (0.145 g, 0.36 mmol) in toluene (2 mL) was added HBF₄ (55 μL of a 54 wt % solution in Et₂O, 0.40 mmol). NH₂(*i*-Pr) was added to the reaction mixture, and complex **4** was obtained as a yellow-brown oily compound after evaporation of the solvent to dryness.

Method B. NH₂(*i*-Pr) (2 μL, 0.02 mmol) was added to an NMR tube filled with a suspension¹⁹ of **2** (0.010 g, 0.02 mmol) in C₆D₆ (0.6 mL). A bleaching of the solution was instantaneously observed, and NMR spectroscopy confirmed that the substitution reaction took place. ¹H NMR (C₆D₆): 0.75–3.40 (m, CH₂CH₂P, NiCH, CH(CH₃)₂, NH₂CH(CH₃)₂, 46H). ¹³C{¹H} NMR (C₆D₆): 17.96 (s, CH(CH₃)₂, 2C), 18.15 (s, CH(CH₃)₂, 2C), 19.51 (s, CH(CH₃)₂, 2C), 19.96 (s, CH(CH₃)₂, 2C), 20.28 (vt, ^vJ_{PC} = 12.5 Hz, CH₂P, 2C), 23.89 (vt, ^vJ_{PC} = 9.1 Hz, CH(CH₃)₂, 2C), 25.33 (vt, ^vJ_{PC} = 8.7 Hz, CH(CH₃)₂, 2C), 25.42 (s, NH₂CH(CH₃)₂, 2C), 38.17 (vt, ^vJ_{PC} = 8.7 Hz, CH₂CH₂P, 2C), 48.47 (t, ²J_{PC} = 8.7 Hz, NiC, 1C), 49.77 (t, ³J_{PC} = 3.8 Hz, NH₂CH(CH₃)₂, 1C). ³¹P{¹H} NMR (C₆D₆): 65.5 (s). ¹⁹F{¹H} NMR (C₆D₆): -149 (br s). Anal. Calcd for C₂₀H₄₆NiP₂F₄NB·H₂O: C, 45.66; H, 9.20; N, 2.66. Found: C, 45.75; H, 9.04; N, 2.76.

[(*i*-Pr)₂PCH₂CH₂]₂CHNi(CO)[BF₄] (5). Method A. To a Schlenk tube containing a solution of complex (PC_{sp₃P^{i-Pr}})NiC≡CMe (0.100 g, 0.25 mmol) in toluene (2 mL) was slowly added HBF₄ (38 μL of a 54 wt % solution in Et₂O, 0.28 mmol). Replacing the N₂ atmosphere with CO led to precipitation of **5** within a few minutes (0.025 g, 21%).

Method B. An NMR tube filled with a suspension¹⁹ of **2** (0.010 g, 0.02 mmol) in C₆D₆ (0.6 mL) was purged with CO (1 atm) for a few minutes, leading to precipitation of **5**.

Method C. A solution of (PC_{sp₃P^{i-Pr}})NiBr (0.100 g, 0.23 mmol) in THF (5 mL) was added to a Schlenk tube containing AgBF₄ (0.057 g, 0.29 mmol), and the reaction mixture was stirred at room temperature for 1 h. The resultant suspension was filtered, and the reaction vessel was purged with CO (1 atm). The color of the solution changed instantaneously, and complex **5** was obtained as a pale yellow powder after evaporation of the solvent to dryness (0.095 g, 88%). ¹H NMR (CDCl₃): 0.60–3.90 (m, CH₂CH₂P, CH(CH₃)₂, NiCH, 13H), 1.33 (m, CH(CH₃)₂, 24H). ¹³C{¹H} NMR (CDCl₃): 18.17 (s, CH(CH₃)₂, 2C), 18.91 (s, CH(CH₃)₂, 2C), 19.36 (s, CH(CH₃)₂, 2C), 19.64 (s, CH(CH₃)₂, 2C), 22.39 (vt, ^vJ_{PC} = 12.6 Hz, CH₂P, 2C), 25.48 (vt, ^vJ_{PC} = 10.3 Hz, CH(CH₃)₂, 2C), 26.52 (vt, ^vJ_{PC} = 9.3 Hz, CH(CH₃)₂, 2C), 38.31 (vt, ^vJ_{PC} = 6.2 Hz, CH₂CH₂P, 2C). (N.B. The NiC signal is presumed to be obscured by the one due to CDCl₃, and the CO resonance was not observed.) ¹³C{¹H} NMR (CD₂Cl₂): 18.32 (s, CH(CH₃)₂, 2C), 19.06 (s,

CH(CH₃)₂, 2C), 19.60 (s, CH(CH₃)₂, 2C), 19.84 (s, CH(CH₃)₂, 2C), 22.79 (vt, ^vJ_{PC} = 12.6 Hz, CH₂P, 2C), 25.91 (vt, ^vJ_{PC} = 12.1 Hz, CH(CH₃)₂, 2C), 27.06 (vt, ^vJ_{PC} = 11.8 Hz, CH(CH₃)₂, 2C), 38.70 (s, CH₂CH₂P, 2C), 77.26 (s, NiC, 1C). ³¹P{¹H} NMR (CDCl₃): 99.1. ³¹P{¹H} NMR (CD₂Cl₂): 99.0. ¹⁹F{¹H} NMR (CD₂Cl₂): -151 (br s). IR (KBr): 2041 cm⁻¹, ν(CO). Anal. Calcd for C₁₈H₃₇NiP₂F₄O₂·H₂O: C, 43.68; H, 7.94. Found: C, 43.53; H, 8.24.

[(Pr₂PCH₂CH₂)₂CH]Ni(OH) (6). To a solution of complex 2 (0.105 g, 0.22 mmol) in C₆H₆ (2 mL) was added KN(SiMe₃)₂ (0.45 mL of a 0.5 M solution in toluene, 0.23 mmol). The solvent was evaporated after 5–10 min, and hexanes was added (5 mL). The resultant suspension was filtered, and crystals of 6 were obtained by concentrating the filtrate to a minimum and keeping the solution at -14 °C for a few hours (0.035 g, 41%). ¹H NMR (C₆D₆): -3.05 (t, ³J_{PH} = 6.1 Hz, NiOH, 1H), 0.80–1.60 (m, CH₂CH₂P, NiCH, 9H), 1.08 (m, CH(CH₃)₂, 6H), 1.23 (m, CH(CH₃)₂, 6H), 1.45 (m, CH(CH₃)₂, 12H), 1.92 (m, CH(CH₃)₂, 4H). ¹H{³¹P} NMR (C₆D₆): -3.05 (s, NiOH, 1H). ¹³C{¹H} NMR (C₆D₆): 17.67 (s, CH(CH₃)₂, 2C), 18.65 (s, CH(CH₃)₂, 2C), 19.33 (vt, ^vJ_{PC} = 3.5 Hz, CH(CH₃)₂, 2C), 19.36 (vt, ^vJ_{PC} = 2.8 Hz, CH(CH₃)₂, 2C), 22.13 (vt, ^vJ_{PC} = 10.7 Hz, CH₂P, 2C), 22.59 (vt, ^vJ_{PC} = 8.6 Hz, CH(CH₃)₂, 2C), 24.42 (vt, ^vJ_{PC} = 7.9 Hz, CH(CH₃)₂, 2C), 38.78 (vt, ^vJ_{PC} = 11.0 Hz, CH₂CH₂P, 2C), 42.15 (t, ²J_{PC} = 11.0 Hz, NiC, 1C). ³¹P{¹H} NMR (C₆D₆): 62.8 (s). Anal. Calcd for C₁₇H₃₈NiOP₂: C, 53.86; H, 10.10. Found: C, 53.39; H, 9.95.

Competition Experiments with HBF₄·Et₂O and HCl·Et₂O.

A NMR tube was filled with an equimolar solution mixture of (PC_{sp3}P^{Pr})NiMe (0.010 g, 0.03 mmol), (PC_{sp3}P^{Pr})NiC≡CMe (0.011 g, 0.03 mmol) and (PC_{sp3}P^{Pr})NiPh (0.012 g, 0.03 mmol) in C₆D₆ (0.6 mL). HBF₄ (4 μL of a 54 wt % solution in Et₂O, 0.03 mmol) was added three times to the tube, and a ³¹P{¹H} NMR spectrum was recorded between each addition. The first spectrum showed the complete disappearance of the peak corresponding to the (PC_{sp3}P^{Pr})NiMe complex, the second one showed the complete disappearance of the (PC_{sp3}P^{Pr})NiC≡CMe complex while the last spectrum showed the complete disappearance of the (PC_{sp3}P^{Pr})NiPh complex. The same experiment was performed with HCl (13 μL of a 2.0 M solution in Et₂O, 0.03 mmol) and displayed the same order of protonation.

Crystal Structure Determinations. Single crystals of 2–6 were grown from a benzene-d₆ (2 and 5) or hexanes solutions at room temperature (3) or at -15 °C (6), or by slow diffusion of hexanes into a saturated solution of the complex in benzene-d₆ (4). The crystallographic data for complexes 2–5 were collected on a Nonius FR591 generator (rotating anode) equipped with a Montel 200 optics, a D8 goniometer, and a Bruker Smart 6000 CCD area detector. The crystallographic data for complex 6 were collected on a Bruker Microstar generator (micro source) equipped with a Helios optics, a Kappa Nonius goniometer, and a Platinum135 detector.

Cell refinement and data reduction were done using SAINT.²⁵ An empirical absorption correction, based on the multiple measure-

ments of equivalent reflections, was applied using the program SADABS.²⁶ The space group was confirmed by XPREP routine²⁷ in the program SHELXTL.²⁸ The structures were solved by direct-methods and refined by full-matrix least-squares and difference Fourier techniques with SHELX-97.²⁹ All non-hydrogen atoms were refined with anisotropic displacement parameters. Hydrogen atoms were set in calculated positions and refined as riding atoms with a common thermal parameter, except for those of the NH₂ and OH moieties of complexes 4 and 6, respectively, which were positioned from residual peaks in the difference Fourier map. Some disorder was taken into account for two positions of the water-coordinated molecule and the BF₄ counterion of 2 (50:50), the β carbons of 2 (50:50), 3 (40:60), and 4 (30:70), in addition for half of the BF₄ moieties of the molecular structure of 5 (50:50). The absolute configuration of the non-centrosymmetric crystals was determined using the Flack parameter.

Acknowledgment. The authors thank Dr. Michel Simard and Ms. Francine Bélanger-Gariépy for their assistance with the resolution of one of the disordered X-ray structures and a referee of this article for the suggestion of performing low-temperature ¹⁹F NMR experiments. We also gratefully acknowledge financial support received from Université de Montréal (fellowships to A.C.) and NSERC of Canada (Discovery and Research Tools grants to D.Z.).

Supporting Information Available: Tables of X-ray data for complexes 2–6 and a graph correlating NMR chemical shift values (³¹P signals for phosphine moieties vs ¹³C signals for the γ-C). This material is available free of charge via the Internet at <http://pubs.acs.org>. Complete details of the X-ray analyses for complexes 2–6 have also been deposited at The Cambridge Crystallographic Data Centre (CCDC 631844 (2), 692059 (3), 692060 (4), 692061 (5), 631845 (6)). These data can be obtained free of charge via www.ccdc.cam.ac.uk/data_request/cif, or by emailing data_request@ccdc.cam.ac.uk, or by contacting The Cambridge Crystallographic Data Centre, 12, Union Road, Cambridge CB2 1EZ, U.K.; fax: +44 1223 336033.

IC801641U

- (25) SAINT, *Integration Software for Single Crystal Data*, Release 6.06; Bruker AXS Inc.: Madison, WI, 1999.
- (26) Sheldrick, G. M. *SADABS, Bruker Area Detector Absorption Corrections*; Bruker AXS Inc.: Madison, WI, 1999.
- (27) XPREP, *X-ray data Preparation and Reciprocal space Exploration Program*, Release 5.10; Bruker AXS Inc.: Madison, WI, 1997.
- (28) SHELXTL, *The Complete Software Package for Single Crystal Structure Determination*, Release 5.10; Bruker AXS Inc.: Madison, WI, 1997.
- (29) (a) Sheldrick, G. M. *SHELXS97, Program for the Solution of Crystal Structures*; University of Göttingen: Göttingen, Germany, 1997. (b) Sheldrick, G. M. *SHELXL97, Program for the Refinement of Crystal Structures*; University of Göttingen: Göttingen, Germany, 1997.